Surface property modifications of silicon carbide ceramic following laser shock peening

Shukla, P, Nath, S, Wang, G, Shen, X & Lawrence, J

Original citation & hyperlink:
Shukla, P, Nath, S, Wang, G, Shen, X & Lawrence, J 2017, 'Surface property modifications of silicon carbide ceramic following laser shock peening' Journal of the European Ceramic Society, vol 37, no. 9, pp. 3027-3038
https://dx.doi.org/10.1016/j.jeurceramsoc.2017.03.005

DOI 10.1016/j.jeurceramsoc.2017.03.005
ISSN 0955-2219
ESSN 1873-619X

Publisher: Elsevier

Surface Property Modifications of Silicon Carbide Ceramic following Laser Shock Peening

Pratik Shukla*[a], Subhasisa Nath[a], Guanjun Wang[b], Xiaojun Shen[c], and Jonathan Lawrence[a]

*[a]Coventry University, Laser Engineering and Manufacturing Group, School of Mechanical, Aerospace and Automotive engineering, Faculty of Engineering, Environment and Computing, Priory Street, Coventry, CV1 5FB, United Kingdom.

[b]Collaborative Innovation Center of Chemistry for Energy Materials, Department of Chemistry, Shanghai Key Laboratory of Molecular Catalysts and Innovative Materials, Fudan University, Shanghai 200433, China

[c]University of Chester, Thornton Science Park, Pool Lane, Ince, Chester, CH2 4NU, United Kingdom

CITATION

Shukla, P., Nath, S., Wang, G., Shen, X. & Lawrence, J. **(**Aug 2017) **Surface property modifications of silicon carbide ceramic following laser shock peening,** Journal of the European Ceramic Society. 37**,** 9**,** p. 3027-3038 12 p.

Abstract

This paper if focused on Laser shock processing (LSP) of silicon carbide (SiC) advanced ceramic. A comprehensive study was undertaken using a pulsed Nd:YAG laser. Surface modifications were investigated, particularly: the roughness, hardness, fracture toughness, microstructure, phase transformation and residual stress induced before and after the LSP surface treatment. The findings showed increase in the surface roughness, changes to the surface morphology, improved hardness, and a reduction in the fracture lengths. The LSP surface treatment also improved the surface fracture toughness from an average of 2.32 MPa.$m^{1/2}$ to an average of 3.29 MPa.$m^{1/2}$. This was attributed to the surface integrity and the induced compressive residual stress as a maximum of -92 MPa was measured compared to an average of +101 MPa on the as-received SiC. A slight change in the surface chemistry was also observed from the XPS spectra, however, no real phase transformation was observed from the X-Ray diffraction analysis. Laser energy density of around 1.057 J/cm^2, 8.5 mm spot size, 10Hz pulse repetition rate (PRR) at 6ns pulse duration, and 1064nm wavelength resulted to obtaining a crack-free surface treatment and demonstrated that the technique is also beneficial to enhance some of the properties to strengthen brittle ceramics such as SiC.

Keywords: Laser Shock Peening; LSP; SiC; Ceramics; Hardness; K_{1c}; Residual Stress; Microstructure, Surface finish; Phase Transformation.

1. Introduction

Laser shock peening (LSP) or laser shock processing has been an applied technique for many years to engineer surface properties of metallic materials [1-4]. This is so because the process offers many benefits such as, improvement in fatigue and hardness; reduced wear rates; increase in compressive stresses just to mention a few. Such benefits have been addressed extensively for metals and alloys over the last two decades [1-5]. With that said, research in LSP of ceramics is rare due to their physical properties inhibiting mechanical yielding and plastic deformation in the same way as it occurs with metals. This is particularly so when ceramics are introduced to intense shock pulse pressure during LSP surface treatment. Therefore, it is not common to obtain the same gains which are conventionally obtained by LSP of metals and alloys. Thus, it is extremely challenging and fruitful to investigate the effects of LSP upon ceramics such as SiC. A successful process to strengthen SiC for machine tool applications for instance could manifest faster spindle speeds, higher feeds rates, with less wear, and have longer operational life. The work in this paper would also enable one to understand the effects of the pulsed laser energy interaction with brittle ceramics such as SiC.

Over two decades of research has been conducted in the area of LSP of metals and alloys [6-11]. Published literature in this area has evolved from the use of micro-second, nano-second to even shorter pulses being applied in both picosecond and femtosecond range on metals and alloys [11-15]. In terms of ceramics, there is very little progress made. Koichi *et.al.* [16], and the preliminary work from the leading author of this study [17] as well as the work of Schnick [18], are the few investigations that exist in the field of LSP of ceramics such as Si_3N_4 and Al_2O_3. Koichi *et.al.* used the Nd:YAG laser at 532nm to laser peen a Si_3N_4 ceramic. Their results reported an increase in surface roughness as the laser irradiance increased. This was reported due to plastic straining as the surface layer of the Si_3N_4 was induced with compressive residual stress with increase in laser irradiance. However, other findings in their work showed reduction in strength, thus, showing inconsistency and contradiction with their results as residual compressive stress in general would indicate surface strengthening leading to a reduction in the flaw size unlike the findings reported by Koichi *et.al*. Bending strength was also reported to be lower than the as-received surface, but showed some inconstancy

between identical samples. Important details such as evidence of the laser shock peened microstructures were not illustrated in their report. Furthermore, Schnick *et. al.* [18] investigated the laser shock processing of Al + SiC particulate composite coatings. The coating was produced using a spray of powders that ranged between 100µm to 500µm over 30 samples. The results showed a modified morphology of the sprayed coatings as the surfaces became smoother and the coatings were less porous. In addition, the process was made to improve wear resistance of high-velocity oxygen fuel sprayed Al + SiC particulate composite coatings.

The motivation of this paper is to examine the surface effects of LSP upon a brittle material such as SiC ceramic by specifically investigating modifications in the hardness, fracture morphology and the microstructure, plane strain fracture toughness (K_{IC}) along with changes in the residual stress, phase transformations using X-Ray Diffraction (XRD) followed by examination of the surface chemistry with the use of XPS. To observe the effects of LSP on SiC, only the laser energy density was changed whilst keeping other parameters constant. This work is a first-step towards developing an LSP technique for SiC based ceramics for applications such as machine tools as well as other industrial ceramics in general. The effects of LSP are investigated to fill the gap in knowledge and will also demonstrate a first-step towards providing a strengthening technique which could improve the service life of industrial ceramics and create new avenue for their applicability, especially where ceramics could replace other materials but are currently restricted to crack sensitivity and low fracture toughness.

2. Experimental Procedures and Analysis

2.1 Material Characterization Methods

2.1.1 Background of the SiC Advanced Ceramic

The SiC ceramic was mechanically and microstructurally characterized prior to all experimentation. The ceramic was cold pressed using isostatic pressing technique (CIP) by Shanghai Unite Technology, China. It was produced with dimensions of 50 x 10 x 5 mm^3 for the LSP experiments (see in Figure 1). The CIP process was conducted

at 455 bar pressure and was sintered at a temperature of 1200˚C for 5 hours. The average grain size was 17.1 µm and ranged from 9 µm to 26 µm over a 100 μm^2 area of the polycrystalline SiC ceramic.

2.1.2 Surface Finish, Hardness Testing and Fracture Toughness Measurements (K_{Ic})

Surface finish was examined using a form Taylor Hobson, Talysurf Series 2, PGI plus - 8nm; Leicester, U.K., for both the as-received and LSP samples. The average as-received surface finish (from 5 samples) was Ra 1.53µm. Indentation tests were carried out with a Vickers macro/micro indentation method using 73.6N indentation load (VHTM 2000; Vickers Ltd. Engineering Group; Sheffield; England). Fracture toughness (K_{Ic}) was determined based on the Vickers indentation technique in relation to our previous work [19-22]. The surface hardness was measured to be 12.50 GPa and the K_{Ic} was determined as 2.31 $MPa.m^{1/2}$.

2.1.3 Microstructural Observations

Following the LSP surface treatment, a detailed observation of the microstructure of the laser shock peened zone was undertaken and all crack lengths found after Vickers hardness tests were observed using optical microscopy and with a scanning electron microscopy ((SEM) SUPRA 40, Zeiss SMT AG; Germany). Both the as-received and the laser shock peened samples were cross-sectioned using a diamond cutter and polished with 600µm, 200µm, 6µm and 1µm polishing cloth for approximately 8mins each so that the cross-sectional microstructure could be examined. The cross-sectional analysis required chemical/thermal etching to reveal the microstructure of the SiC ceramic. The etching process adopted the use of Murakami reagent at boiling temperatures (approximately 200°C) for about 30mins in a high temperature furnace.

2.1.4 Compositional Analysis

Samples were analyzed for elemental change in the surface and near-surface regions using X-ray photoelectron spectroscopy (XPS) and scanning electron microscopy-energy dispersive X-ray (SEM-EDX) measurements were made using a silicon drift detector system (X-Act with INCA software, Leo 1455VP SEM,

Oxford Instruments; U.K.). The XPS analyses were performed using a bespoke ultra-high vacuum chamber fitted with Specs GmbH Phoibos 150 analyzer, Focus 500 monochromater and F20 charge neutralizing gun. Spectra were acquired using the Al monochromatic source, 1486.6 eV X-ray energy with an analysis area approximately 2mm diameter. The SiC ceramic was also analyzed for elemental change in the surface and near-surface regions using XPS and SEM-EDX prior to and after the LSP surface treatment.

2.1.5 Phase Transformation and Residual Stress Analysis

A detailed analysis of the phase evolution was carried out by x-ray diffraction (XRD) technique (Bruker D8 Discover, Germany) with Cu Kα radiation (wavelength ≈ 0.15418 nm) at a scanning speed of 0.02°/s. The X-ray source was operated at an accelerating voltage of 40kV and current of 25mA. The size-strain plot (SSP) method was used to calculate the crystallite size, strain, and stress on the as-received SiC surface and laser shock peened SiC based on previous methodology of Bindu and Thomas [23]. The SSP method has a significant advantage over other methods, so that less importance is given to the high angle peaks and it is assumed that the "strain profile" is characterized by a Gaussian function. The "crystallite size" is characterized by a Lorentzian function [23]. Hence, the SSP approximation is:

$$(d_{hkl}\, B_{hkl}\, cos\theta_{hkl})^2 = \frac{1}{V_s}\,(d_{hkl}^2\, B_{hkl} \cos\theta_{hkl}) + (\frac{\varepsilon}{2})^2 \qquad (1)\ [23]$$

where d_{hkl} is the interplanar distance between (hkl) planes, β_{hkl} is the full width half maximum of the peak at a particular (hkl) which was obtained after subtracting from the instrumental broadening, V_s=(3/4)D_v (where D_v is the crystallite size), and ε is the apparent strain. The crystallite size and strain were calculated from the slope and intercept of the plot between $(d_{hkl}\beta_{hkl}\cos\theta_{hkl})^2$Vs $(d^2_{hkl}\beta_{hkl}\cos\theta_{hkl})$, where $(d_{hkl}\beta_{hkl}\cos\theta_{hkl})^2$ was plotted on the Y-axis and $(d^2_{hkl}\beta_{hkl}\cos\theta_{hkl})$ on the X-axis.

Residual stress on the laser shock peened and untreated zones were also measured using the XRD technique (d Vs $\sin^2\Psi$ technique) by application of a stress Goniometer attached to a Bragg Brentano Diffractometer

(Bruker D8 Discover; Germany). The X-ray source was operated at an accelerating voltage of 40kV and current of 25mA. The measurement of stress on the SiC samples was performed using Cu Kα radiation with a step size of 0.01° and time per step of 10s. In this method, θ/2θ scans corresponding to a particular reflection were conducted at various tilt angles ψ (0, 5, 10, 15, 20, 25, 30, 35, 40, and 45), where ψ is the angle between the sample normal and the diffraction vector. For the calculation of residual stress, the (304) plane of SiC phase at~ 133.3° was considered.

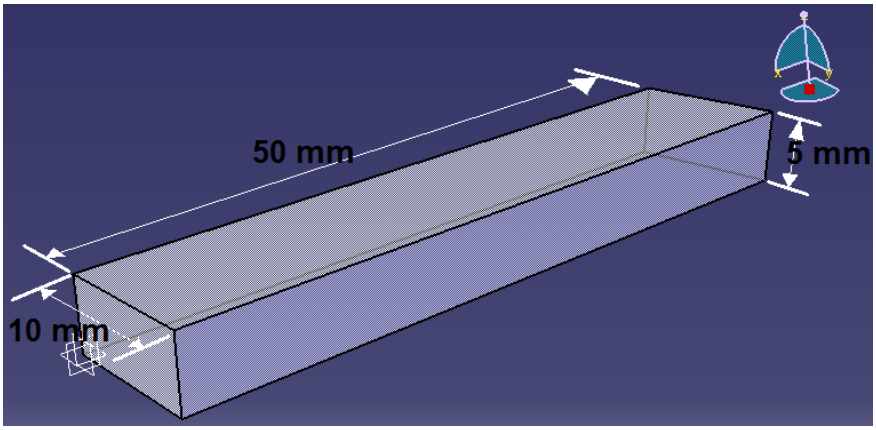

Figure 1. A schematic of the SiC ceramic used for laser shock processing surface treatment.

2.2 Laser Shock Processing Surface Treatment

A pulsed laser (Continuum; Powerlite; DLS 8000; San Jose; USA) was used for the experimental study herein and is shown in Figure 2. The laser emitted a wavelength of 1064nm and was applied with an energy density ranging from a minimum of 0.379J/cm^2 to a maximum of 1.702J/cm^2. The laser delivered 6ns long pulse with a repetition rate of 10Hz. This was done by generating a single shot to the surface of the SiC in order to investigate the LSP effects on the tool-grade SiC for the first-time. The profile of the laser was top-hat and its far field divergence was 0.45mrad. A large spot diameter of 8.5mm was used so that the energy density is focused on a large surface area, thus, avoiding the possibility of generating any potential cracks that may result from thermal shock. The footprint of the beam was taken on 8.5mm spot on a laser burn paper prior to conducting the main experiments. The laser emitted a radiance density of 0.83 to 2.36 (J/mm^2/Sr^{-1}), per pulse as calculated using our previous methodology published elsewhere [24]. All the experiments are made with single pulse. This was because it was the very first investigation which had made in-roads into this field. In addition, over-lapping

would increase the thermal shock that would be introduced into the material so in order to understand the laser material interaction during LSP, it was essential that the effects of a single pulse, without any overlaps is first investigated and understood. Further studies are underway to determine the ideal pulse over-lap. The treatment was conducted using atmospheric condition. In addition, LSP was conducted using a black polyethylene (PE) tape as an absorptive surface layer over the material and a water layer of about 1 to 2 mm thickness was made to flow over the SiC surface. Conventionally, both ablative and the confinement layers were known to bring about the obvious benefits to the components part [25]. Five samples were used for the experiments in order to evaluate the effect of LSP on the SiC ceramic. Laser energy was recorded using an energy meter which enabled the measurement of the energy fluctuations of ± 3mJ, recorder for 30 sec duration. Table 1 show laser energy density delivered to the surface of the SiC ceramic during the LSP surface treatment with its effects created on the material at the respective energy densities that were applied.

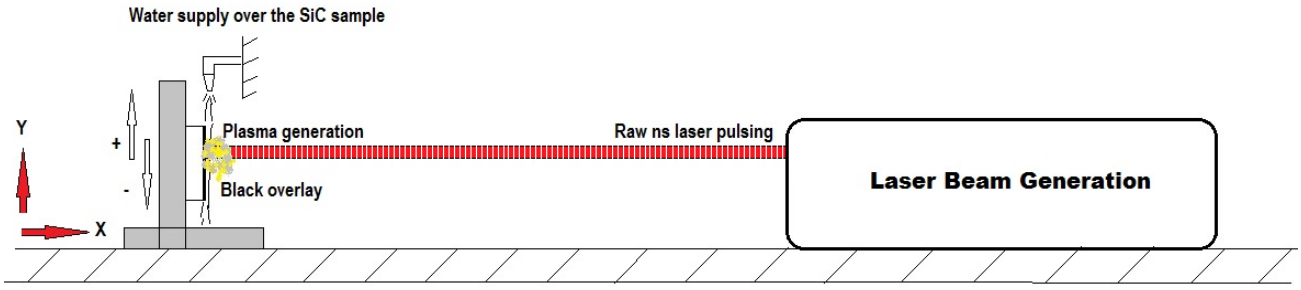

Figure 2 A schematic of the laser beam delivery and the experimental set-up of LSP SiC ceramic.

Table 1. The laser energy densities and its effects when delivered to the SiC ceramic during LSP using an 8.5mm Spot size, 6ns pulse duration and 10 Hz frequency.

Laser Energy Density (J/cm^2)	Effect on SiC
0 (Untreated)	Some porous zones evident
0.379	Evidence of laser beam foot print
1.057	Laser foot-print became distinct
1.702	Porosity formation in various zones

2.3 Hugoniot Elastic Limit in Relation to Laser Shock Processing Parameters

One of the well-known aspects about the LSP process is that the plasma pressure created by the laser pulse must exceed the Hugoniot Elastic Limit (HEL) of the material so that sufficient deformation could occur. The HEL is classified as the peak stress which a solid could withstand in one-dimensional shock compression as the laser beam interacts with the solid. This is when deformation could occur which is reversible at the particular shock wave front [26]. In the present work, the plasma pressure is first identified and calculated using equations (2). This equation was used as an estimation rather than an accurate calculation. For accurate calculation, more sophisticated numerical model can be employed to evaluate the pressure of the plasma [40, 46, 47]. However, a simpler model was sufficient for this work [34], and the use of sophisticated models were beyond the scope of this work.

$$P_{max}(GPa) = 0.01\sqrt{\frac{\alpha}{2\alpha+3}}\sqrt{Z}\sqrt{I_0} \quad (2)\ [27]$$

Where Pmax is the maximum peak pressure induced by the plasma in GPa (See Table 2); α is the ratio of thermal to internal energy which was 0.1; Z is the reduced shock impedance between the SiC and confinement medium (water) in our case (926000). I_0 is the constant absorbed laser power density in the confined ablation mode given elsewhere [27 - 34]. This was determined using the [27 – 34] and is presented in Table 2. So the model of the plastic deformation due to the shock wave produced by the LSP surface treatment can be determined by Equation (3):

$$HEL = \frac{1-\nu}{1-2\nu}\sigma_y^d \quad (3)\ [34]$$

Where ν is the Poisson's ratio of the material (0.14 for SiC ceramic), σ_y^d is the dynamic yield strength at high strain rates. Furthermore, as the shock wave propagates into the material (usually the case for metals), plastic deformation occurs up to a depth at which the peak stress induced on the material would equal to its HEL. The HEL is related to the dynamic yield strength at high strain rates, σ_y^d according to [27 - 34]. The values were determined for the LSP of SiC ceramic using both equation (2) and (3) to determine the plasma pressure and the HEL for the LSP conditions applied in this work (see Table 2).

On account of previous literature, it can be assumed that the increase in hardness would decrease the dynamic yield strength [35]. The static yield strength of the SiC used in this work was 21 GPa, whilst the dynamic yield strength would decrease to about 7 GPa based on previous literature stating that the dynamic yield strength is reduced during the material interaction with the laser [44]. This equated to HEL of the SiC to be 26.90 GPa owing to the dynamic strength of 21 GPa and HEL of 8.96 GPa as per the static yield strength being 7 GPa. In both cases, the pressure at various laser energies and intensities was far too low and was not sufficient enough (see Table 2) to exceed the HEL, and render the material to plastically deform. Additionally, it should be further noted that only light pressure was introduced so that a crack-free surface was produced. In addition, the laser energies adopted in this research were maximum capacity that the laser system could deliver.

Upon increasing the laser intensity would enable the generation of enough plasma pressure for the material to exceed the HEL; at the same time, working under the fracture threshold of the SiC ceramic. Furthermore, we would like to emphasize that, since no residual stress can be derived by the shock wave traveling along the materials due to the processing conditions being far from the SiC yield limit, it was still possible to obtain encouraging results, namely; residual stress backed by microstructural changes as well as an increase in hardness and fracture toughness. Due to the existing knowledge, we speculate that the change in composition could have caused the increase in compressive residual stress despite the laser parameters not yielding to sufficient shock pulse pressure. The XPS spectra and the values in Table 4 in particular showed increase in C content of 19.6%, a rise in O content of 49% as well as a reduction in the Si by 83%. These changes could be the predominant drivers in increasing the hardness, fracture toughness, as well as the compressive stress as further shown in this paper. The work of Khor *et.al.* [48], showed that oxidation improved the mechanical properties. In addition, two types of oxidation effects that could be found on SiC ceramic - either an active or a passive oxidation, as stated by Roy *et.al.* [49]. The former was reported to reduce the strength of the ceramic and the latter on the other hand improved the strength with respect to weight gain as the SiO_2 layer was formed which was the case in the laser shock peened SiC herein. Moreover, the C content has increased after LSP. This could also be attributed to carbon hardening, as well as the enhancement in dislocations density that created

low level of plastic or elastic + plastic deformation, leading to not only improved fracture toughness but also compressive residual stress despite the shock pulse pressure being low from the applied laser parameter.

Table 2 Presents values of both pressure and HEL for the parameters applied for this work.

Laser Energy (mJ)	Laser Intensity - I_0 (Gw/cm^2)	Plasma Pressure (GPa)
215	0.063	0.427
600	0.1763	0.7136
800	0.235	0.8246
966	0.2838	0.904

Note: All calculations are based on the following parameters: pulse duration 6ns; frequency 10Hz; Spot Size 8.5 mm, dynamic yield strength of 7GPa for SiC [35] and static yield strength 26.90 GPa, Poisson's ratio of a SiC is 0.18.

3. Results and Discussion

3.1 SiC Microstructure Evaluation after Laser Shock Processing

The as-received surface in some areas showed evidence of machining marks such as striations, and micro-pores and voids as illustrated from Figure 3 of the SEM micrograph of the SiC as-received surface. Figure 4(a) showed an optical image of the 8.5 mm diameter laser spot exhibited on the SiC ceramic. With increasing laser energy density, the spot diameter became more evident on the surface of the ceramic. Using higher laser energy in the range of 1.410J/cm^2 to 1.702J/cm^2, it was possible to see the maximum footprint of the beam as shown in Figure 4(b). After further increase in the laser energy density, the effect on the SiC ceramic became somewhat distinct as shown in Figure 5(a) to (d). This was particularly evident when the laser shock peened surfaces were compared to the as-received surface in Figure 4(b). With increasing laser energy density, as the SiC surface was treated with LSP, the machining marks and striations were no longer apparent. A considerable level of machining marks were initially present on the as-received surface that were eliminated after LSP. This goes to show that the LSP surface treatment modified the surface integrity which was also confirmed by the measured asperities. Particularly, 1.498J/cm^2 and 1.702J/cm^2 resulted to considerable microstructural change. This in turn opened some surface pores at 1.410J/cm^2 to 1.702J/cm^2 energy density. At low laser energy density

(0.379J/cm^2), not a remarkable microstructural change was apparent as seen in Figure 5(a). However, one can see that pre-existing surface defects were eliminated as the energy density was increased to 1.057J/cm^2, 1.410J/cm^2, and finally to 1.702J/cm^2 (see Figure 5 (a-d)). With that said, the opening of pores, and voids (at maximum laser energy) could be attributed to the laser pulse ablating some of the material, thus, exposing the surface defects. This indicated that defect-free surface and undesirable features could be readily obtained using energy density of around 1.057J/cm^2, and by applying aforementioned conditions. At the same time, energy density beyond 1.057J/cm^2 may not be desirable for LSP of SiC ceramic, on account of our applied conditions, as it seems to produce some ablation during laser material interaction. Thus, it is suggested that the results found at the energy density of 1.057J/cm^2 were more suitable for conducting LSP operation to engineer the surface respectively.

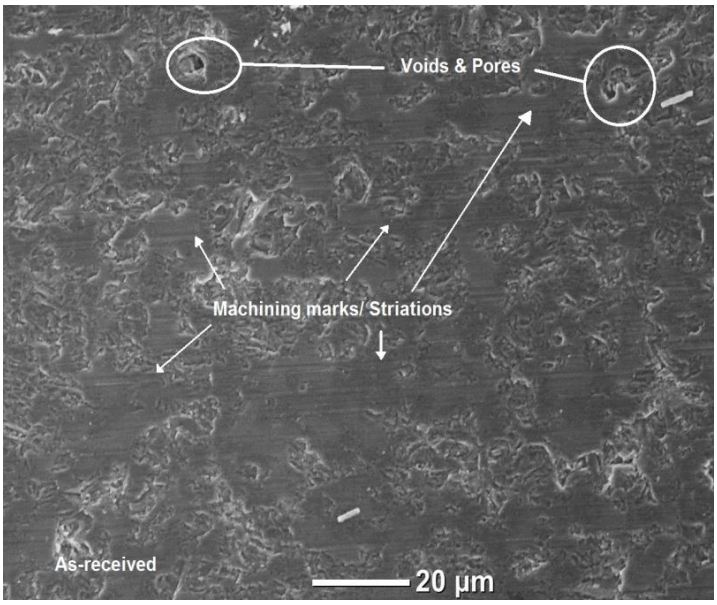

Figure 3. As-received SEM micrograph of the SiC ceramic.

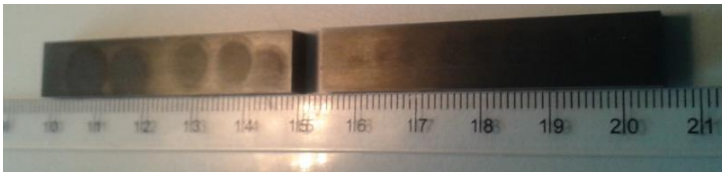

(a)

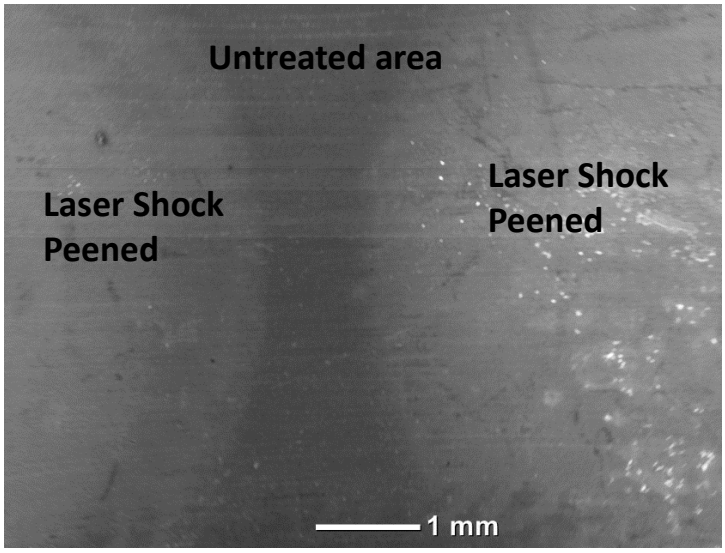

(b)

Figure 4. Optical and SEM images of the SiC ceramic with distributed pulses in (a); and (b) LSP conducted at 1.702J/cm^2, 10Hz, for 6ns pulse duration with a single pulse.

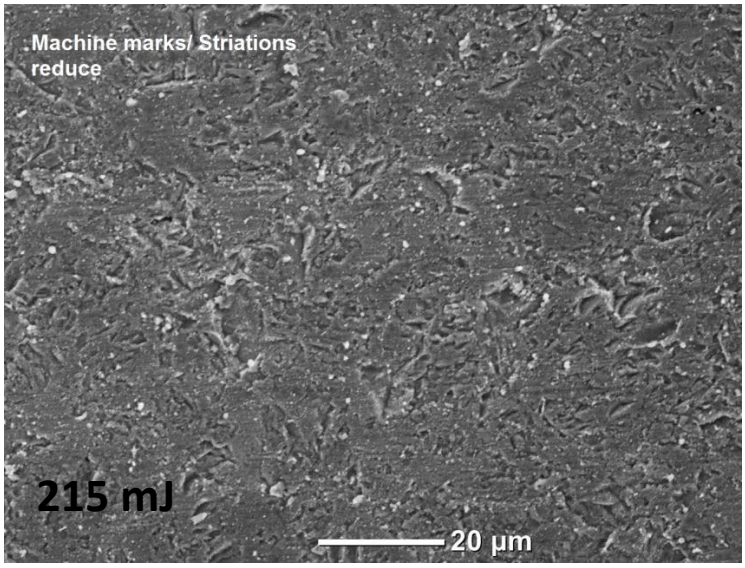

(a)

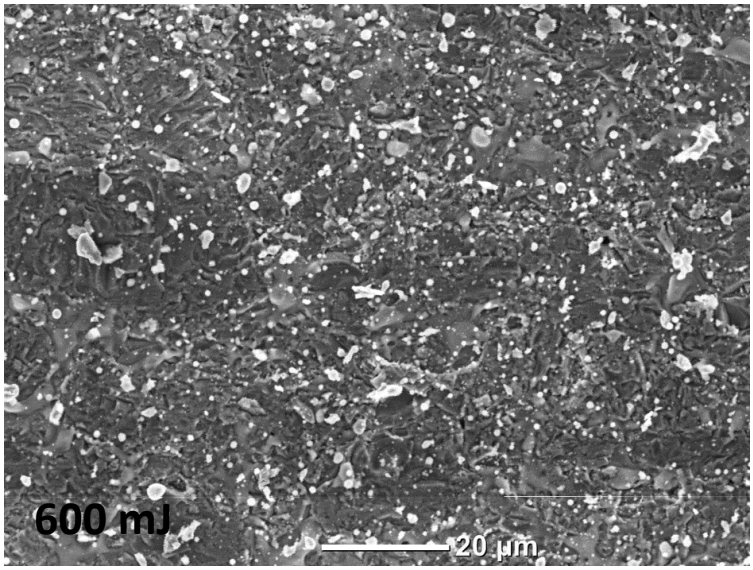

(b)

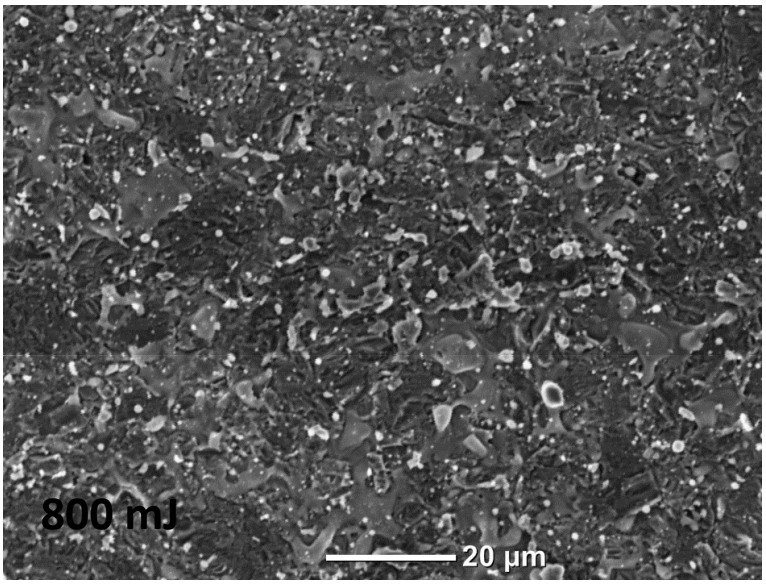

(c)

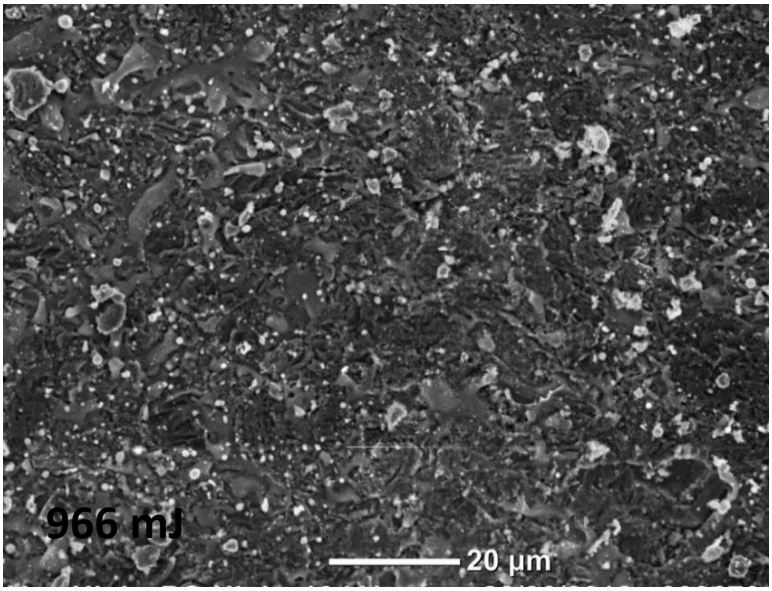

(d)

Figure 5 SEM micrograph of the laser shock peened SiC ceramic at 0.379J/cm^2 in (a); 1.057 J/cm^2 in (b); 1.410 J/cm^2 in (c); and 1.702J/cm^2 in (d), around the centre of the spot.

Figure 6 showed the cross-sectional microstructure of the as-received SiC ceramic in (a), LSPned SiC with laser energy density of 0.379 J/cm^2 in (b), LSP SiC with laser energy density of 1.057 J/cm^2 in (c), and (d) the LSP of SiC with laser energy density of 1.702 J/cm^2. Presence of two phase microstructure was evident from the microstructure of as-received SiC ceramic and LSP SiC ceramics. EDS analysis, as shown in Figure 7, revealed that the light phase was rich in Si and C and the dark phase was rich in Si. Thus, from EDS analysis, it was concluded that the light phase is SiC and the dark phase is the untreated Si. The near surface region showed no signature of melting which can be seen from Figure 6 (b) and (c). During LSP of SiC ceramics, a black polyethylene tape was used as an absorbent which prevented the surface of the SiC ceramic from being melted. The absorbent layer allowed the laser energy to pass through the surface of SiC ceramic in form of shock waves. Changes in the microstructure (grain refinement, precipitate formation, micro-crack formation etc.) in metallic systems due to laser shock peening have been reported previously [38 - 41]. A close comparison between the microstructures of the untreated SiC ceramic and LSP of SiC ceramics revealed no significant difference due to increase in laser

energy as shown in Figure 6(a) to (d). The laser energy densities which transported into the SiC ceramic in form of shock waves was unable to cause any visible microstructural change.

The shock waves are responsible for the low level plastic deformation in the near surface region of the material in the form of increased dislocation density, which changed the microstructure of the material in the near surface region. It is believed that due to the presence of significantly less plastic deformation (or low dislocation density) in LSP SiC ceramics, no visible microstructural changes were observed. To understand the effect of LSP on the formation dislocation, XRD peak profile analysis was conducted and is presented in section 3.7.1.

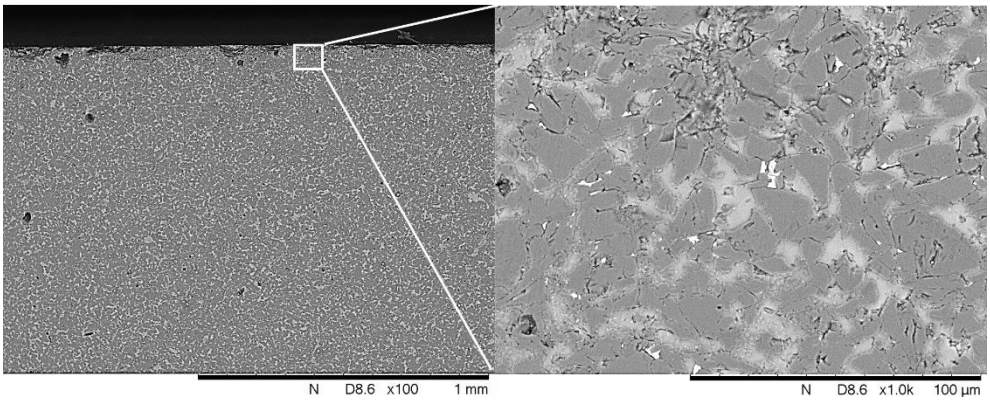

(a)

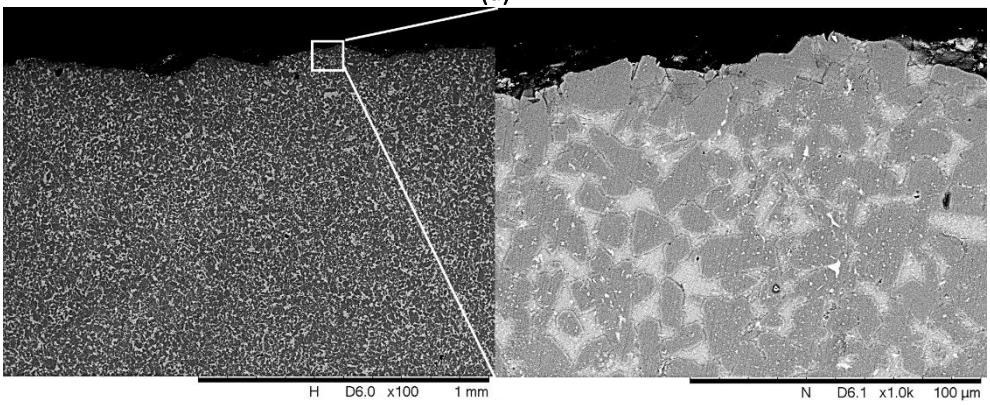

(b)

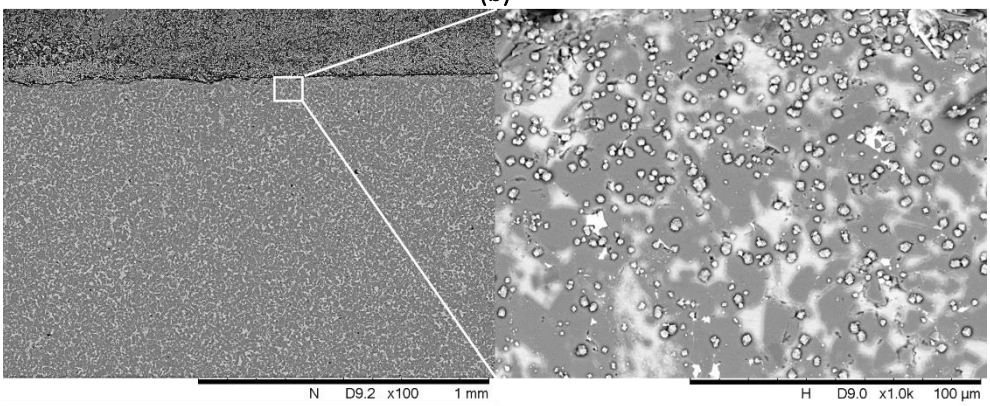

(c)

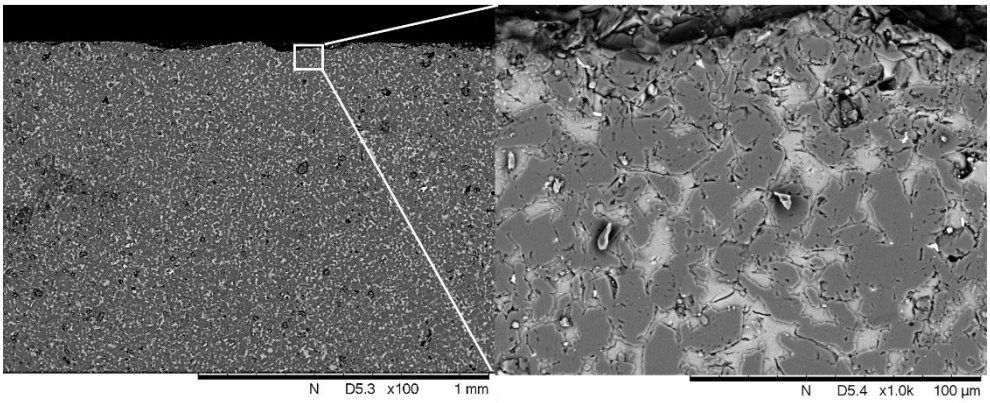

(d)

Figure 6 SEM micrographs of cross-section of untreated SiC in (a), LSP SiC with laser energy density of 0.379 J/cm^2 in (b), LSP SiC with laser energy density of 1.057 J/cm^2 in (c), and LSP SiC with laser energy density of 1.702 J/cm^2 in (d).

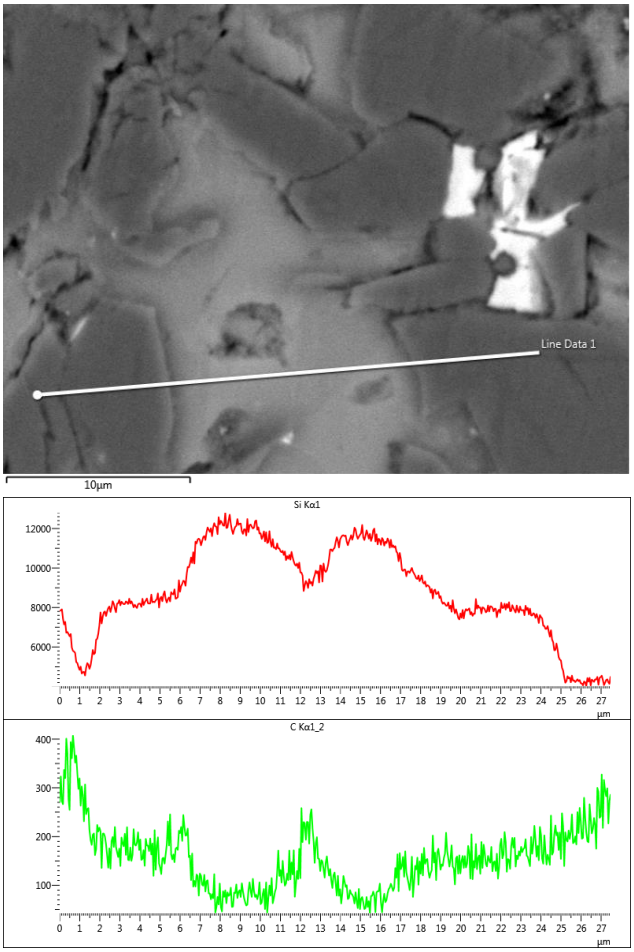

Figure 7 SEM of some light phase was rich in Si and C and the dark phase rich in Si in (a), and (b) the Energy disperive X-ray (EDX) spectroscopic analysis of the untreated SiC ceramic zone.

3.2 Topographical Effects

The surface measurements were conducted over five individual sample of SiC and were compared with the as received surface. The average surface roughness (Ra) over five samples was measured to be 1.55µm for the as-received SiC (see Table 3). The average Ra value for the laser shock peened surfaces peaked to 5.30µm as shown in Table 3. This is generally expected with LSP of metallic materials so it is reasonable to assume it will be so for ceramics and could also be predicted/tailored, based on the material removal phenomena during laser pulse processing. The surface roughness and material removal increased with increasing laser energy density, particularly for SiC/Si_3N_4 ceramic systems [44]. This is generally thought to be the case until ablation, melting, vaporization begins to take place [36, 37], naturally, increasing the waviness and in turn the roughness. However, this was not the case herein (melting and vaporization), as further evident from the microstructure which showed changes in the material integrity, ultimately, leading to roughening of the laser shock peened SiC ceramic. This caused the laser shock peened surface to change roughness from Ra of 1.55µm (as-received) to 2.50 µm at 0.379 J/cm^2, 3.51µm at 1.057 J/cm^2 and 5.30µm at J/cm^2, respectively as shown in Table 3 and Figure 8.

Table 3. The average surface roughness of the SiC as-received and the laser shock peened surfaces of the SiC ceramic.

Surfaces	As-received 0 J/cm^2	Laser shock processing @ 0.379 J/cm^2	Laser shock processing @ 1.057 J/cm^2	Laser shock processing @ 1.702 J/cm^2
Average Surface Roughness (Ra)	1.55 µm	3.50 µm	4.35 µm	5.30 µm

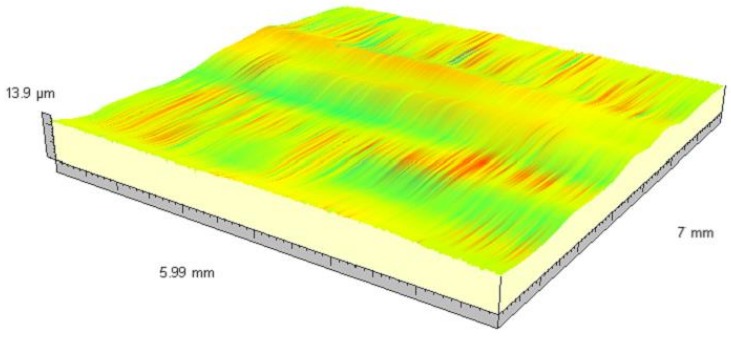

(a)

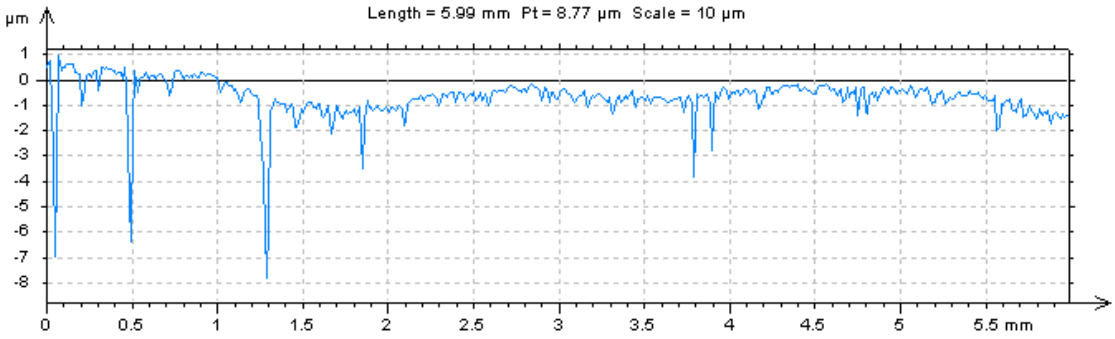

(b)

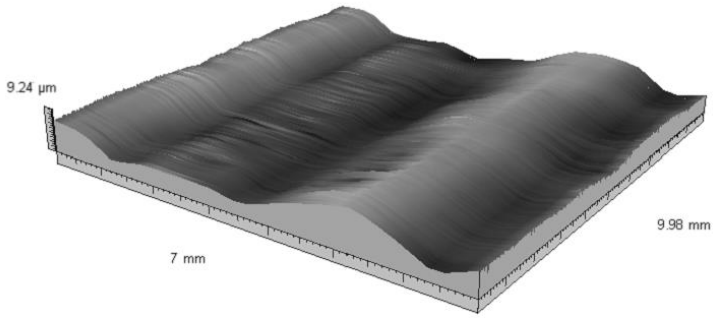

(c)

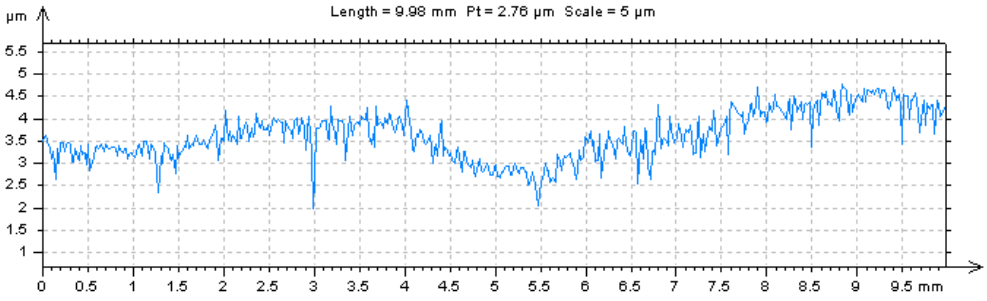

(d)

Figure 8 Roughness of the as-received SiC ceramic surface profile in (a and b), and the laser shock peened surface applied 1.057 J/cm^2 in (b and c).

3.3 Phase Transformation

3.3.1 Phase Analysis by X-Ray Diffraction

LSP is a high strain rate processing technique, where there is a chance of alteration of phase and microstructure of the sample from its original state (although not always common). Figure 9 showed the x-ray diffraction scans of the as-received SiC (plot 1) and laser shock peened SiC with energy densities 0.379 J/cm^2 (plot 2), 1.057 J/cm^2 (plot 3), and 1.702 J/cm^2 (plot 4). Presence of cubic SiC as a major phase and hexagonal SiC along with few

unreacted Si as minor phases were evident from Figure 9. It was also evident from Figure 9 that there was no phase transformation or formation of new phases as-results of LSP surface treatment. It was observed that the cross-sectional microstructure of the SiC ceramics was unaffected by the LSP surface treatment (see Figure 6). Similarly, it was also observed from Figure 9 that LSP has no effect on the phase structure with these particular parameters applied to the SiC ceramic. It was believed that the applied laser energy densities were not sufficient to generate significant plastic deformation or increased dislocation density to cause changes in phase and microstructure of the SiC. However, the original intention behind application of LSP is to induce compressive stress on the material surface without altering its phase or microstructure. So, the range of parameters studied here were acceptable keeping in mind no change in phase and microstructure was observed.

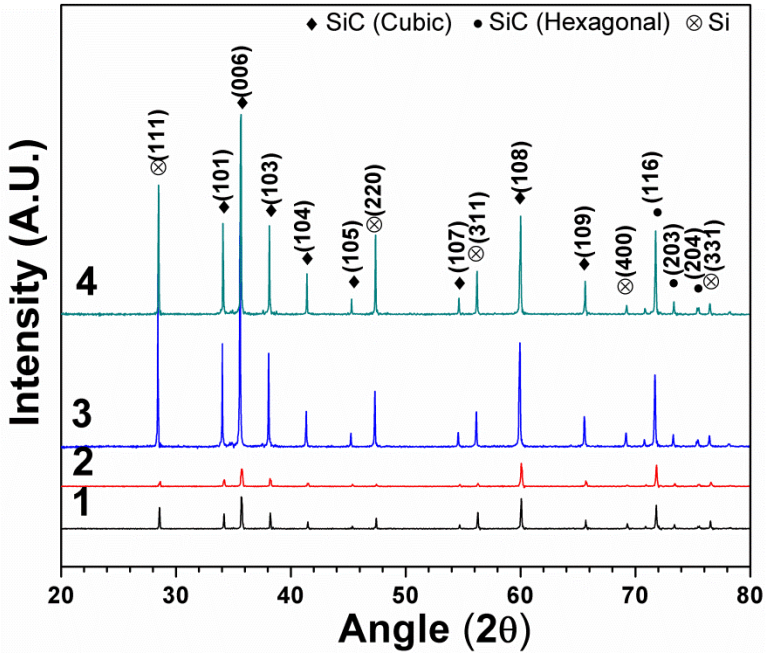

Figure 9 X-ray diffraction scans of untreated SiC (plot 1) and laser peened SiC with laser energy densities of 0.379 J/cm^2(plot 2), 1.057J/cm^2(plot 3), and 1.702 J/cm^2(plot 4).

The peak broadening analysis of the (304) plane was undertaken to understand the effect of LSP surface treatment on the development of plastic strain as shown in Figure 10. The peak broadening was not so significant between the LSP SiC ceramic and as-received SiC, as evident from Figure 10. A careful examination

of the peaks revealed that a slight increase in peak broadening associated with LSP of SiC ceramics had occured. This implied development of plastic strain of very less magnitude due to LSP of SiC ceramics within the studied parameters.

A similar analysis was done by Akita *et.al.* [16], to understand the effect of LSP on the diffraction peak broadening of Si_3N_4. They observed a significant peak broadening after LSP which they attributed to increase in dislocation density. It was previously observed that shot peening by mechanical impact could also increase dislocation density on the surface of the ceramic [42]. Thus, it is understood that the selected range of laser energy densities were not sufficient to introduce significant amount plastic deformation on the surface of SiC ceramics, but that is a significant finding in its own right as a first-time study of LSP of SiC ceramics.

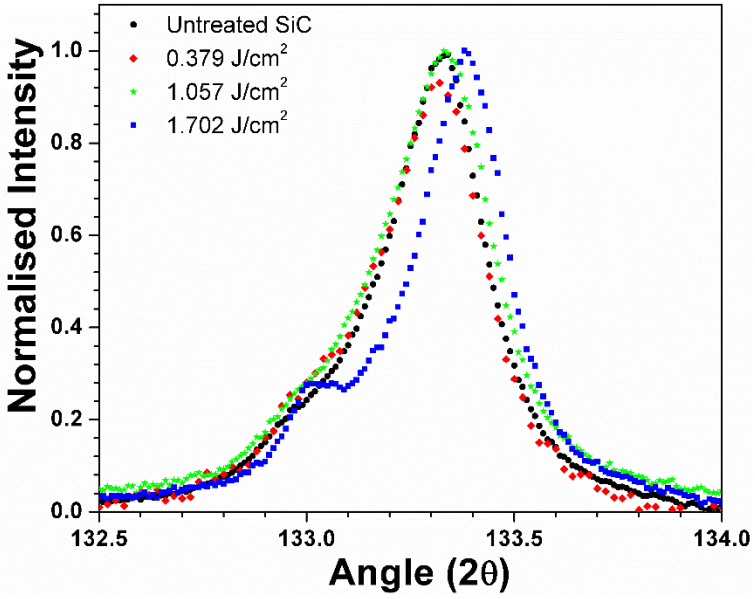

Figure 10 X-ray diffraction scans of SiC phase for the (304) plane at different laser energy densities.

3.3.2 Phase Transformation with Respect to Elemental and Compositional Changes Post Laser Shock Processing

Since no real phase transformation was observed from the XRD analysis was an indication that the results ought to be verified by other techniques such as elemental and compositional change that may have taken place as further shown. The results of surface elemental analysis by SEM-EDX and by using the XPS for the as-received and the LSP surface treatment are shown in Table 4. The XPS measurements reflect the composition of the outermost few nano meters of the sample, typically up to 10 nm (at maximum), whereas, the SEM-EDX results were from a much greater depth of approximately 1μm. The SEM-EDX data from the untreated reference sample show a composition similar to that except for bulk SiC, with a small percentage of the Si replacing O (i.e. a slightly oxidized surface) and weak evidence for a possible carbon-rich surface layer. The LSP surface treatment caused relatively little difference in the SEM-EDX results, with only a small increase in O and a small decrease in C found. The XPS data from the untreated reference sample, with its much enhanced surface sensitivity compared to the SEM-EDX, showed a composition consisting of an oxidized surface hydrocarbon layer typical of that found on material exposed to the normal laboratory environment, overlying a bulk SiC ceramic. After LSP, the XPS data showed a strong increase in the amounts of surface C and O, and a reduction in the amount of Si. This is indicative of the formation of an oxidized carbon-rich surface layer, although, only in the region of 10 nm depth. In general, the LSP surface treatment also resulted in a lower overall level of minor species. The changes in the surface chemistry were apparent from changes in the line-shapes of the XPS C 1s and Si 2p peaks as shown in Figure 11 (a) to (d). The carbon 1s XPS spectrum from the as-received untreated reference surface (Figure 11 (a)), showed a low binding energy component due to carbon in carbide bonds. It also showed a major component due to C-C bonded carbon, probably hydrocarbon contamination typical of air-exposed surfaces, with additional minor components at higher binding energies due to carbon in single- and double-bonded oxygen-containing groups. The corresponding Si 2p spectrum (Figure 11 (c)) showed a major component due to Si in SiC, and a weaker contribution from oxidized SiC. The corresponding spectra after LSP surface treatment were significantly altered. The carbide component of the carbon peak (Figure 11 (b)) was

only just visible, and the carbon spectrum was dominated by C-C bonds and by carbon in C-O bonds. The Si spectrum (Figure 11 (d)) was much reduced in intensity, reflecting the much lower level of Si detected by XPS on this surface, and showed components due to oxidized SiC and to elemental Si, along with a weak contribution from Si in SiC. These results indicate transformation of the surface from that of SiC with the expected level of surface contamination of an air-exposed material, to a surface with a high carbon and oxygen content indicative of an oxidized and possibly graphitized surface with some elemental Si present. The LSP surface treatment appeared to have resulted in breakdown of the SiC to Si and C, both of which became partially oxidized in the process. The change in the surface chemistry of the SiC ceramic was not detrimental but was sufficient to bring about a change in the microstructure. In addition, this could have also led to a reduction the residual stress as well as the increase in hardness found over the surface of the laser shock peened SiC. Therefore, the modification of hardness, K_{Ic} and the reduction in flaw size and possibly the indentation of compressive residual stress could be closely linked with these microstructural alterations as well as induction of compression on the top surface layer of the laser shock peened region from the generated shock waves during the LSP surface treatment.

Table 4. Summary of the surface compositions in atom % determined by XPS and by SEM-EDX for the as-received reference and the LSP SiC ceramic. In all cases, the balance to 100 atom% was made up of low level species including Cl, K, Ca, Fe, Cu and Zn.

	Composition (atom %)			
	As-received Surfaces		Laser Peened Surfaces	
Element	**XPS**	**SEM-EDX**	**XPS**	**SEM-EDX**
C	55.3	52.0	66.1	50.1
Si	18.5	46.7	2.4	46.8
O	19.1	1.1	28.1	2.8
N	1.6	-	1.3	-
Na	1.7	0.08	0.6	-
Al	1.3	-	0.01	-

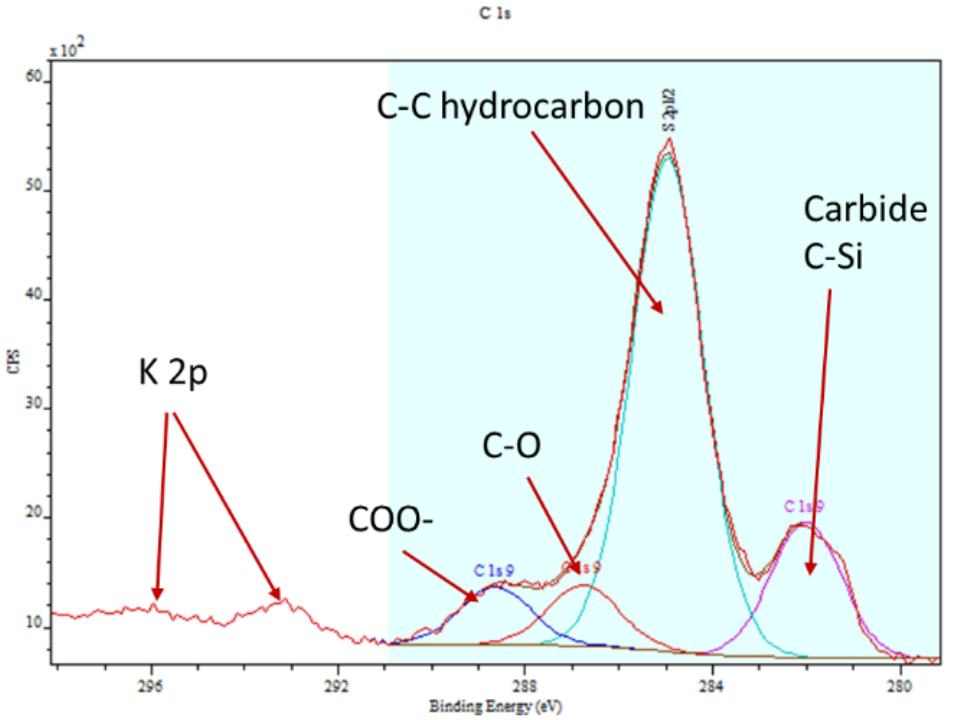
C 1s
x 10^2
C-C hydrocarbon
Carbide
C-Si
K 2p
C-O
COO-
CPS
Binding Energy (eV)

(a)

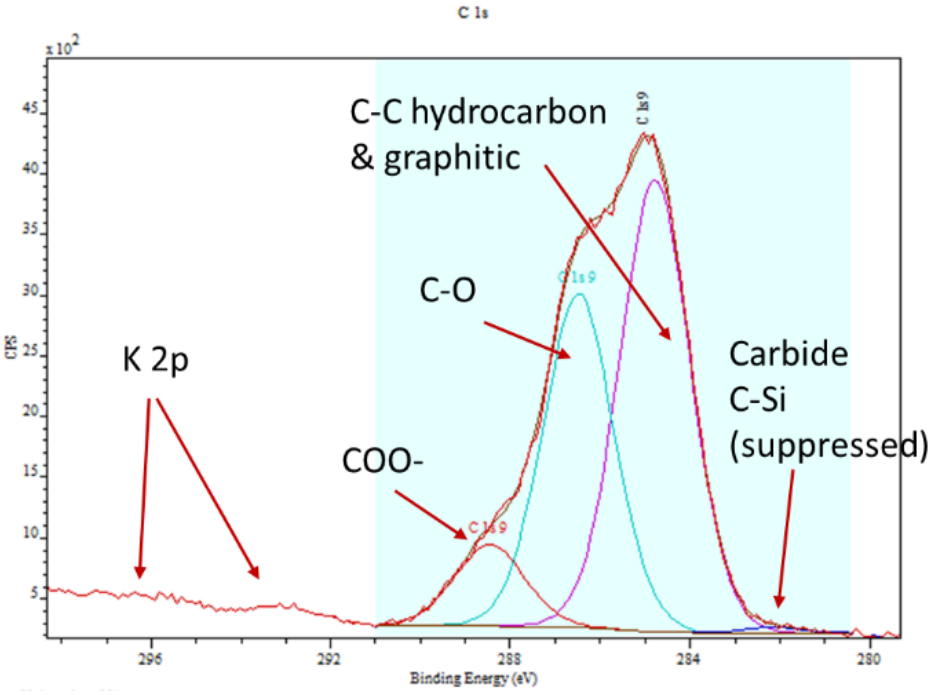
C 1s
x 10^2
C-C hydrocarbon
& graphitic
C-O
K 2p
COO-
Carbide
C-Si
(suppressed)
CPS
Binding Energy (eV)

(b)

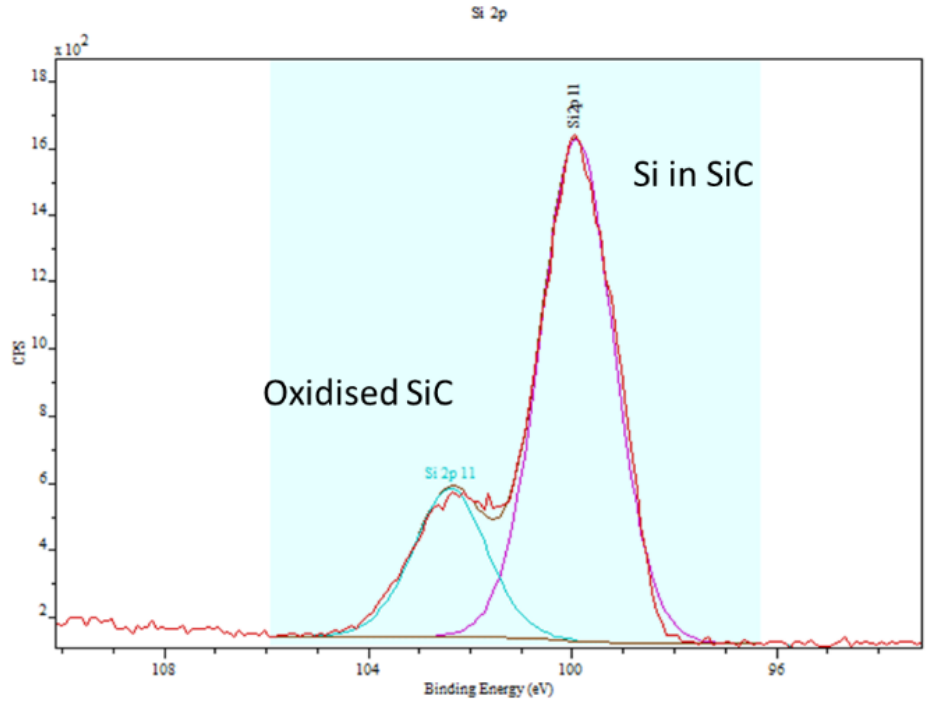

(c)

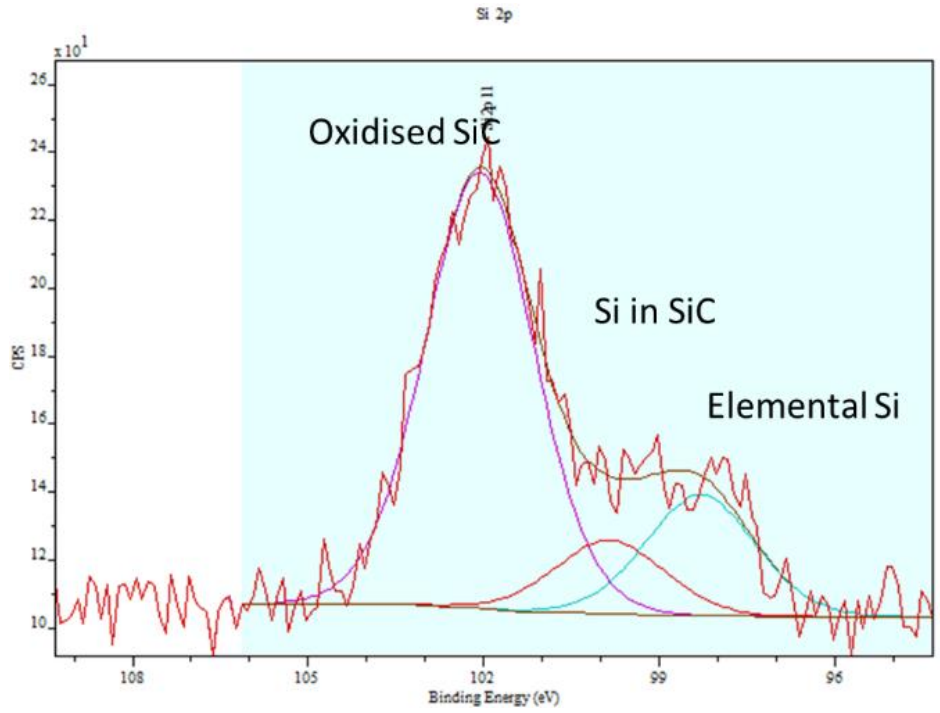

(d)

Figure 11. C 1s spectra from the as-received and laser shock peened SiC surfaces respectively in (a) and (b); and (c) and (d) using the Si 2p spectra from the untreated and laser shock peened SiC surfaces respectively.

3.4 Stress and Strain Measurements

3.4.1 Size-Strain Plot Analysis

Table 5 summarizes the crystallite size and micro-strain measured on the untreated laser shock peened SiC ceramics under different parameters. Comparing the values of micro-strain for both the treated and untreated surfaces in Table 5, it was observed that the micro-strain in the LSP SiC ceramic was lower than the untreated SiC. A decreased micro-strain in the LSP SiC ceramic was attributed to the strain relaxation due to LSP. With increase in the laser energy density had increased the micro-strain up to 1.23 $\times 10^{-4}$, which indicated a generation of plastic deformation. It is well known that LSP has been used to introduce plastic deformation on the surface of metallic materials which in turn improves the mechanical properties significantly [33]. However, the micro-strains in all the SiC samples were of same order of magnitude which implies less plastic deformation due to LSP under the studied parameters.

From Table 5, it was observed that the crystallite size was initially decreased and then increased with the rise in laser energy density. Decrease in grain size due to LSP of aluminium alloy was reported by Lu *et.al.* [42]. The observed grain refinement that was due to transformation of dislocation tangles to sub-grain boundaries as a result of high strain rates followed by dynamic recrystallization of these sub-grain boundaries to form refined microstructure. However, in the present case it was believed that due to the presence of low plastic deformation, the above mentioned mechanism is not applicable. The reason behind the increase in crystallite size is under further investigation. It should be noted that a standard deviation associated with each measurement has been calculated and subsequently presented in Table 5. The software used for analysis of this data was Origin 8 platform in order to fit XRD peak profiles. All the fitting showed R^2 values well above 99%.

Table 5 Geometric parameters for the as-received and laser shock peened SiC ceramic with changes in the power density.

Sample Type J/Cm^2	Crystallite Size (μm)	Strain (×10^{-4})
0	1.65 ± 0.03	1.85
0.379	1.55 ± 0.09	1.23
1.057	1.61 ± 0.04	1.4
1.702	1.80 ± 0.07	1.5

3.4.2 Residual Stress Measurements

Table 6 summarizes the residual stress developed on the surface of the as-received SiC ceramic and laser shock peened SiC ceramic. From Table 6, it is evident that LSP surface treatment significantly altered the residual stress state from tensile (as-received) to compressive (after LSP). The development of residual stress on the surface of SiC samples depend on the amount of laser energy delivered on to the surface as well as its ability to generate plastic deformation. Table 6 revealed that with increase in laser energy density from 0 J/cm^2 to 1.702 J/cm^2, the residual stress changed from +101 MPa (tensile stress) to -97 (compressive stress), respectively. This was a reduction of 198 MPa and was in increase by almost 2 folds. The introduction of compressive residual stress on the surface of SiC after LSP would enhance their mechanical properties such as hardness, K_{Ic}, and the reduction found in the Vickers diamond indentations, and its respective crack lengths that resulted from induced compressive residual stress. Secondly, other properties such as wear resistance, fatigue performance and bending strength would also improve from this type of surface treatment.

Table 6 Residual stress on both the as-received laser shock peened SiC ceramic.

Sample Type J/cm^2	Residual stress (MPa)
0	101 ± 16
0.379	51 ± 11
1.057	-92 ± 9
1.702	-97 ± 7.5

3.5 Indentation Evaluation Post Laser Shock Processing

The as-received surface of the SiC ceramic comprised of 12.50 GPa of hardness from an average of 10 Vickers indentation tests and so it was characteristic that the footprint of the Vickers indentation was measured at an average of 212µm and the respective crack length from tip-to-tip were measured to be 217µm (see Figure 12), with a possible error of ±10%. This was also taken from undergoing 10 individual indentation tests. Up on increasing the laser energy density resulted in Vickers diamond footprints that were reduced by an average of 12µm at 0.379J/cm^2, 44µm at 1.057J/cm^2 and 32µm for 1.702J/cm^2 of laser irradiation respectively. Nevertheless, the findings demonstrated that using LSP surface treatment increased the surface hardness of the SiC. This meant that the footprint of the diamond indentations were also reducing due to hardening of near surface layer when compared to the as-received surface. This is attributed to the compressive residual stress induced into the ceramic after LSP as evidenced from the residual stress analysis in section 3.4.2.

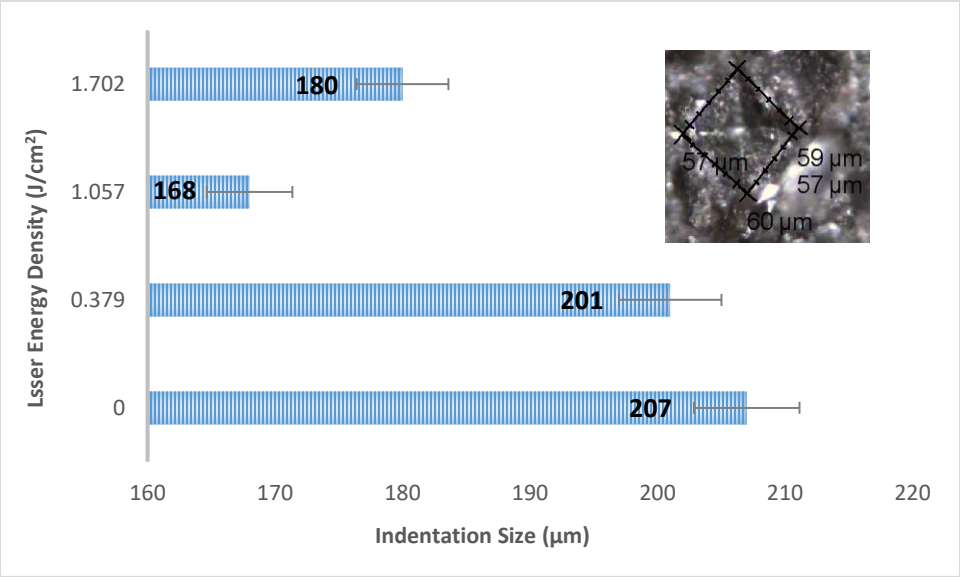

Figure 12 A graphical illustration showing Vickers indentation size of both the as-received (0 J/cm^2) and the laser shock peened surfaces of SiC ceramic. The diamond indentation foot-print accompanied by the graph demonstrate the size of the diamond foot-print.

3.6 Hardness and Crack Length Post Laser Shock Processing

The crack lengths of the diamond indents produced on the laser shock peened surfaces were also considerably smaller when compared to the as-received surface as shown in Figure 13(a). On average the crack lengths were 217µm for the as-received SiC, and comparatively, the crack lengths of the laser shock peened surfaces had reduced with increasing laser energy density. The lowest flaw size found was 152µm, which indicated that the surface became less prone to cracking and showed resistance against diamond impact despite the measured hardness to have shown significant increase. This inherently was an indication that there was an increase in the brittleness of the top/near surface layer. This meant that the surface should be more prone to cracking after the LSP surface treatment. However, the crack lengths were reduced in size from tip-to-tip which also showed that there was induction of some compressive stress. This in turn prevented the cracks from expanding, whilst being indented by the Vickers indentation. In order to investigate this further, a residual stress study was carried-out comparing the as-received residual stress state and the LSP induced residual stress of the SiC ceramic. This was confirmed later by the induced compressive stress. The Vickers diamond footprints also reduced in size considerably as previously stated which indicated that harder surface responded less in

comparison to the softer surface during the Vickers indentation test. The hardness of the laser peened surfaces was measured to a maximum of 19.98 GPa at 1.057 J/cm^2, and then 16.45 GPa at 1.702 J/cm^2 as shown in Figure 13(b). In terms of future study, it is suggested that the focus on the rationale for the change in hardness from 19.98 GPa to 16.45 GPa at 1.057 J/cm^2 and 1.702 J/cm^2 should be given. Thus, it is postulated based on the microstructural evaluation, the energy induced at 1.702 J/cm^2 had created zones that would have covered some of the porous regions but less uniformly. This indicated that the ideal laser energy density would be around 1.057J/cm^2 to bring about the best possible increase in hardness to the SiC ceramic compared to the laser shock peened surface at 1.410 J/cm^2 and 1.702J/cm^2. Overall, the findings from this work showed a level of strengthening of the SiC ceramics as it had become less prone to cracking and yielded a good response to Vickers indentation load impact of 73.6N when compared to the as-received surface of the SiC ceramic due to the induced residual compressive stress from the LSP surface treatment.

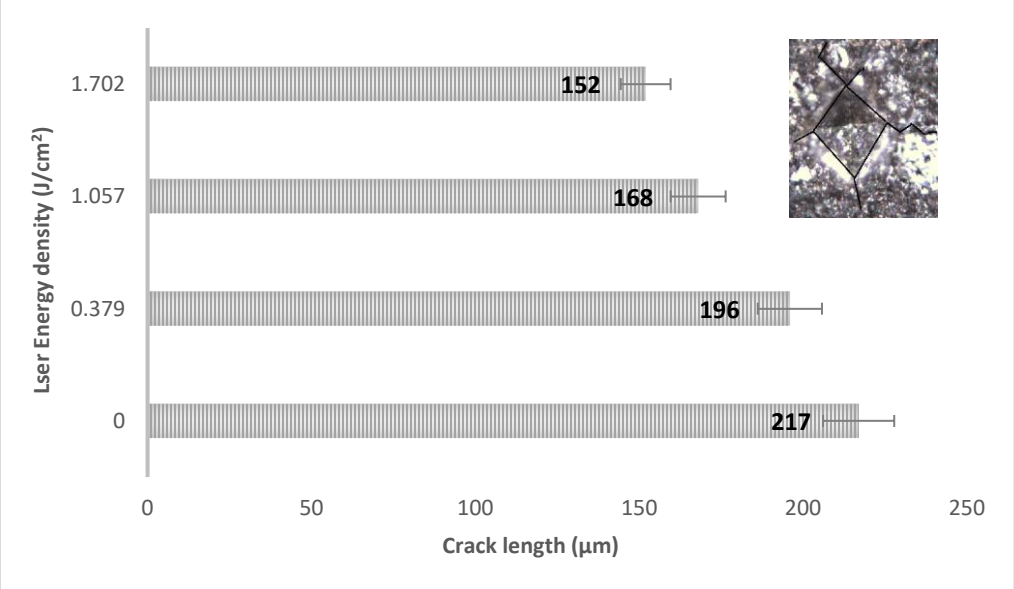

(a)

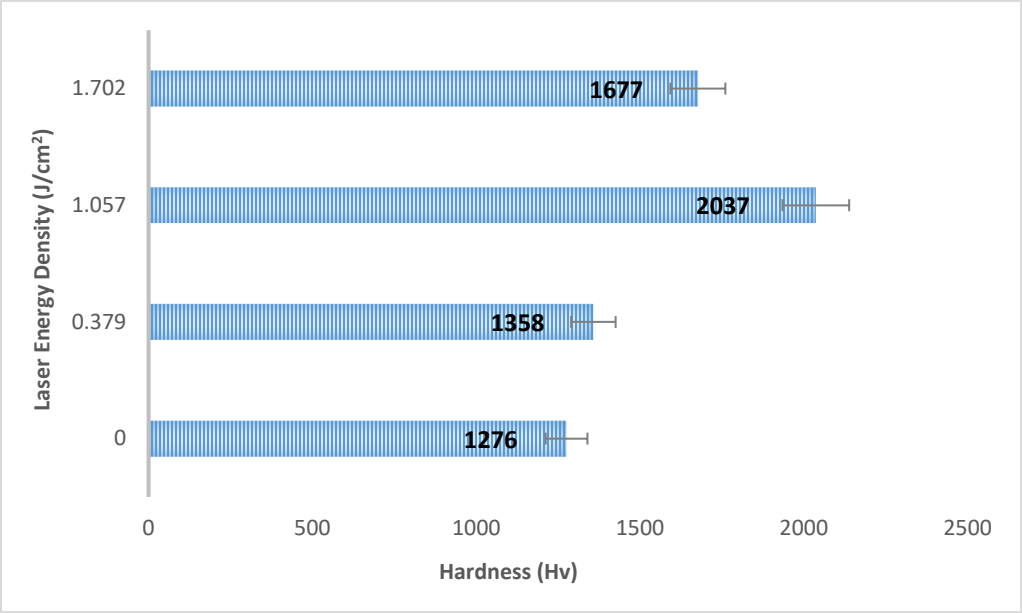

(b)

Figure 13 The change in flaw size in (a); and (b) the change in hardness for both the as-received (0 J/cm2) and the laser shock peened surfaces of SiC ceramic applied at various energy densities.

3.7 Fracture Toughness (K_{Ic}) Parameter Post Laser Shock Processing

Figure 14 shows the comparison between fracture toughness parameter K_{Ic} of the as-received surface and the laser shock peened surface at various energy densities of the SiC ceramic. The comparisons show an increase in K_{Ic} from 2.32 MPa.m$^{1/2}$ for the as-received surface (0 J/cm^2) to 2.60 MPa.m$^{1/2}$, at 0.379J/cm^2 and 3.29 MPa.m$^{1/2}$ at 1.702J/cm^2 respectively for the laser shock peened surfaces. This demonstrated that the hardness, the crack length and the K_{Ic} could be altered to suite a specific surface requirement. This could be done upon optimizing the laser energy density and the associated parameters. On this more, the rise in hardness and the K_{Ic} could be attributed to the fact that an increase in residual compressive stress layer during LSP surface treatment and forming a path for increasing the dislocation motion may have resulted. Through this mechanism, a level of elastic + plastic deformation at the sub-micron level could have yielded to result to a better indentation response under the loading of the Vickers indentation diamond. As such, this resulted to reduction in the crack length and the indentation size of the diamond, as the acting tensile stress of the Vickers indenter would have to overcome the induced compressive stress under the laser peened area. But due to the induced compression, it was indicative that further loading would have to be applied to extend the flaw size,

and since the opposite effect took place, a rise in the surface K_{Ic} occurred under the applied conditions. This prediction would deem positive upon further analysis of the residual stress state under the laser peened area, as well as analyzing the cross-sectional residual stress state on the top surface layer.

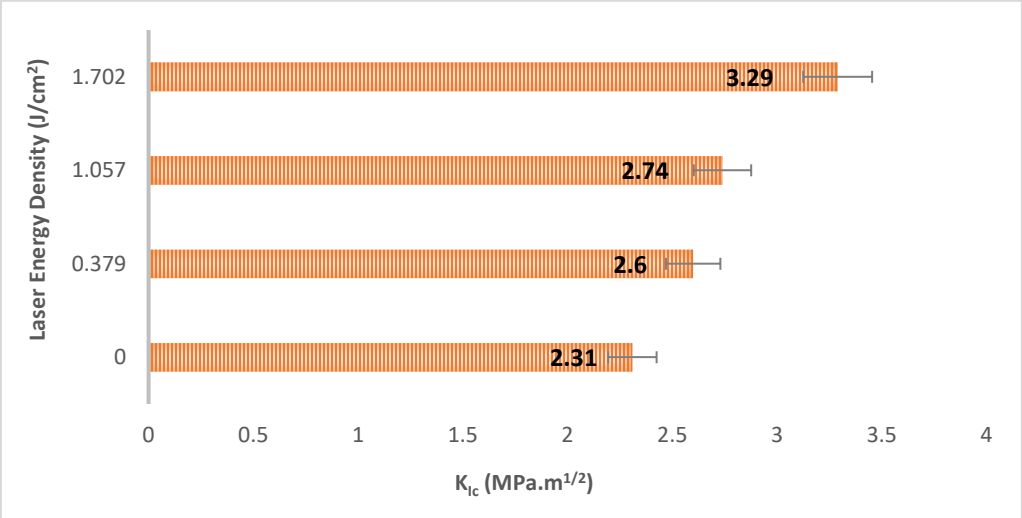

Figure 14 The fracture toughness parameter (K_{Ic}) for both the as-received (0 J/cm^2) and the laser shock peened surfaces at different laser energy densities applied to the SiC ceramics.

4. Conclusions

This work is focused on the examination of surface properties of SiC ceramic following LSP surface treatment. It is a preliminary investigation reporting some of the very first findings in the field of LSP ceramics, particularly, applied to a brittle ceramic such as a SiC. The results have shown that it is possible to control the ceramic's surface roughness, microstructure, hardness, crack geometry, K_{Ic} and the induced residual stress by applying required laser energy and appropriate LSP parameters. Upon further work, the process could prove to be effective for enhancing the performance and functional life of many industrial ceramic parts. In particular, the results of this work showed an increase in surface roughness after LSP compared to the as-received surface. This indicated a change in surface integrity at sub-micron level at the highest applied laser energy. Considerable microstructural modification also occurred on the laser shock peened surfaces as pre-existing surface defects were eliminated with increasing laser power, but surface pores and voids were exposed at the highest laser energy applied in various areas of the SiC ceramic. This goes to show that the suitable laser energy for LSP would

be around 1.057J/cm^2, with 8.5mm spot size, 10Hz PRR delivered in 6ns. The hardness was increased from 12.50 GPa to 19.98 GPa on the laser shock peened zone at 1.057J/cm^2, whist the hardness reduced to 16.45 GPa at 1.702J/cm^2. Nonetheless, all laser peened surfaces revealed an increase in hardness and a reduction in the diamond footprints from the Vickers indentation test. Moreover, the lengths of the flaws of the diamond indentation footprints were also reduced. This shows that the laser shock peened SiC ceramic responded better under mechanical loading in comparison to the as-received SiC. In addition, an increase in K_{Ic} also resulted after LSP from 2.32 MPa.m$^{1/2}$ to a 3.29 MPa.m$^{1/2}$, under the applied conditions. Both the increase in hardness, a reduction in the flaw size and the increase in the surface K_{Ic} indicated that the laser shock peened surface may have undergone a level of plastic + elastic deformation as confirmed from the 2 folds increase in the residual stress (- 198 MPa) compared to the as-received SiC. This in turn, generated a compressive stress layer under the peened area and prevented a deeper and broader penetration of the diamond footprint and expansion of the resulting crack lengths. No such phase transformation was observed from the XRD analysis, however, a compositional change was observed. We believe that further refinement of the laser parameters could render further improvement in the aforementioned material properties and have a possibility of generating deeper and higher compressive stress that is a key factor in such a surface modification technique.

5. Acknowledgement

The leading author of this paper would like to thank the Engineering Physical Sciences Research Council (EPSRC) for funding the former laser loan pool scheme and also the Science & Technology Facilities Council (STFC) for supporting a new system for laser shock peening applications (Grant no: EP/G03088X/1, (13250017 - NSL4)), which was made and deployed for the first-time in relation to this research on a broader scale.

6. References

1. M. Gerland, M. Hallouin, N.H. Presles, Comparison of two new surface treatment processes, laser induced shock waves and primary explosive: application to fatigue behavior, Materials Science and Engineering: A. 156(2), (1992)175-182.

2. J. E. Masse, G. Barreau, Laser generation of stress waves in metal, Surface and Coatings Technology. 70 (2–3), (1995) 231-234.

3. P. Peyre, P. Merrien, P.H. Lieurade, and R. Fabbro, Laser induced shock wave surface treatment for 7075-T7351 aluminium alloys, Surface Engineering. 11(1), (1995) 47 – 52.

4. A. H. Clauer, Laser shock peening for fatigue resistance in surface treatment of titanium alloys, The Metal Society of AIME Conference. (1996) 217-230.

5. Y. Sano, N. Mukai, K. Okazaki, M. Obata, Residual stress improvement in metal surface by underwater laser irradiation, Nuclear Instruments and Methods in Physics Research Section B: Beam Interactions with Materials and Atoms. 121 (1–4), (1997) 432-436.

6. P.P. Shukla, T.P. Swanson, J.C. Page, Laser Shock Peening and Mechanical Shot Peening Processes Applicable for the Surface Treatment of Technical Grade Ceramics: A Review, Proceedings of the Institution of Mechanical Engineers Part B: Journal of Engineering Manufacture. 228 (5), (2014) 639-652.

7. H. Chen, W.J. Kysar, and Y.Y. Lawrence, Characterization of plastic deformation induced by micro-scale laser shock peening," Journal of Applied Mechanics (ASME). 71, (2004) 713- 723.

8. S. Kalainathan, S. Sathyajith, and S. Swaroop, Effect of laser shot peening without coating on the surface properties and corrosion behavior of 316L steel, Optics and Lasers in Engineering. 50(12), (2012) 1740 - 1745.

9. S.Q. Jiang, J.Z. Zhou, Y.J. Fan, S. Huang, S. and J.F. Zhao, Prediction on Residual Stress and Fatigue Life of Magnesium Alloy Treated by Laser Shot Peening, Advances in Materials Manufacturing Science and Technology XII, Vol 1: Advanced Manufacturing Technology and equipment and Manufacturing Systems and Automation, Materials Science Forum. 626-627, (2009) 393-398.

10. R.S. Mannava, S. Bhamare, V. Chaswal, L. Felon, D. Kirschman, D. Lahrman, R. Tenaglia, D. Qian, and V. Vasudevan, Application of laser shock peening for spinal implant rods. International Journal of Structural Integrity, 1757-9864, (2010).

11. W. Steen, J. Mazumder, Laser Material Processing, Fourth Edition. Springer-Verlag Publication Ltd: London (2010).

12. Y.K. Gao, Improvement of fatigue property in 7050 – T7451 aluminium alloy by laser peening and shot peening, Material Science and Engineering A. 528, (2011) 3823 – 3828.

13. I. Goran, Advances in Laser Shock Peening Theory and Practice around the World, 2(1): Emerald Group Publishing Limited, Bingley: United Kingdom (2011).

14. L. Dongkyun, Feasibility Study on Laser Micro welding and Laser Shock Peening Using Femtosecond Laser Pulses, Biblio Bazaar, LLC, Charleston, South Carolina, USA (2011).

15. L. Dongkyun, Feasibility study on laser microwelding and laser shock peening using femtosecond laser pulses, Doctoral Thesis, The University of Michigan, U.S.A, (2011).

16. A. Koichi, Y. Sano, T, Kazuma, T, Hirotomo, I.O. Shin, Strengthening of Si_3N_4 Ceramics by Laser Peening," Residual Stresses VII, ECRS7. 524 – 525, (2006) 141-146.

17. P. Shukla, G.C. Smith, D.G. Waugh, J. Lawrence, Development in Laser Peening of Advanced Ceramics, Proceedings of the SPIE. 9657, (2015) 77-85.

18. T. Schnick, S. Tondu, P. Peyre, L. Pawlowski, S. Steinhäuser, B. Wielage, U. Hofmann, and E. Bartnicki, Laser Shock Processing of Al-SiC Composite Coatings, Journal of Thermal Spray Technology. 8(2), (1999), 296 – 300.

19. P.P. Shukla, J. Lawrence, Fracture toughness modification by using a fibre laser surface treatment of a silicon nitride engineering ceramic. Journal of Materials Science. 45 (23), (2010), 6540-6555.

20. P.P. Shukla, J. Lawrence, H. Wu, On the fracture toughness of a Zirconia engineering ceramic and the effects thereon of surface processing with fibre laser radiation. Proceedings of the Institution of Mechanical Engineers, Part B, Journal of Engineering Manufacture. 224 (B10), (2010), 1555-1570.

21. P.P. Shukla, J. Lawrence, Evaluation of fracture toughness of ZrO_2 and Si_3N_4 engineering ceramics following CO_2 and fibre laser surface treatment. Optics and Lasers in Engineering. 49(2), (2011), 229 - 239.

22. P. Shukla, Viability and Characterization of the Laser Surface Treatment of Engineering ceramics. A doctoral thesis: Loughborough University. U.K (2011).

23. P. Bindu, S, Thomas, Estimation of lattice strain in ZnO nanoparticles: X-ray peak profile analysis, Journal of Theoretical Applied Physics. 8, (2014), 123–134.

24. P. Shukla, J. Lawrence, Y. Zhang, (2015), Understanding laser beam brightness: A review and new prospective in material processing, Optics and Laser Processing, 75, 40–51.

25. A.H. Clauer, T.C. Walters, S.C. Ford, The Effects of Laser Shock Processing on the Fatigue Properties of 2024-T3 Aluminum, Lasers in Materials Processing, (Metals Park, OH: ASM International), 7 (1983).

26. R.A. Graham, Solids under High-Pressure Shock Compression, Mechanics, Physics and Chemistry, Springer-Verlag New York (1993).

27. J. H. Kim and J. W. Lee, Effects of Simulation Parameters on Residual Stresses in 3D Finite Element Laser Shock Peening Analysis, Global Journal of Researches in Engineering, Mechanical and Mechanics Engineering. 13 (9), 2013, 1 – 10.

28. K, Ding, and L, Ye, Laser shock peening Performance and process simulation, CRC Press. pp. 47-118, (2006).

29. K. Ding, and L. Ye, Simulation of multiple laser shock peening of a 35CD4 steel alloy, Journal of Materials, Processing Technology. 178, (2006), 162-169.

30. W. Braisted, R. Brockman, Finite element simulation of laser shock peening, International Journal of Fatigue. 21, (1999), 719-724.

31. X. Ling, W. Peng, G. Ma, Influence of Laser Peening Parameters on Residual Stress. Field of 304 Stainless Steel. Journal of Pressure Vessel Technology. 130, (021120), (2008), 1-8.

32. P. Peyre, R. Fabbro, Laser shock processing: a review of the physics and applications, Optical and Quantum Electronics. 27, (1995), 1213-1229.

33. C. Yang, P.D. Hodgson, Q. Liu, L. Ye, Geometrical effects on residual stresses in 7050-T7451 aluminum alloy rods subject to laser shock peening, Journal of Material Processing Technology. 201, (2008), 303 - 309, 2008.

34. A. K. Gujba, M. Medraj, Laser Peening Process and Its Impact on Materials Properties in Comparison with Shot Peening and Ultrasonic Impact Peening, Materials, 7, (2014), 7925 – 7974.

35. R.M. Davies, The Determination of Static Dynamic Yield stresses using a steel ball, Proceedings of the Royal Society A, Mathematical, Physical and Engineering Sciences. 197, 1050, (1949), 1471 - 2946.

36. R.K. Edwards, P.S. Edwardson,C. Carey, G. Dearden, K.G. Watkins, Laser micro peen forming without a tamping layer, International Journal of Advance Manufacturing Technology. Vol? (2009), PP.

37. A. Tamhankar, and R. Patel, Use of Short Pulse Width Laser for Maximum Material Removal Rate, The 29th International Congress on Applications of Lasers and Electro-Optics (ICALEO 2011). Laser Materials Processing. 23 – 27. October 2011. Orlando. FL. USA. Paper No. M601. Laser Institute of America.

38. A. Salimianrizi, E. Foroozmehr, M. Badrossamay, H. Farrokhpour, Effect of Laser Shock Peening on surface properties and residual stress of Al6061-T6, Optics and Lasers in Engineering. 77, (2016), 112–117.

39. Y. Hua, Z. Rong, Y. Ye, K. Chen, R. Chen, Q. Xue, H. Liu, Laser shock processing effects on isothermal oxidation resistance of GH586 super alloy, Applied Surface Science. 330, (2015), 439–444.

40. Y. Chang, Y. Liao, S. Suslov, D. Lin, G. J. Cheng, Ultrahigh dense and gradient nano-precipitates generated by warm laser shock peening for combination of high strength and ductility, Materials Science & Engineering. A609, (2014), 195–203.

41. J.Z. Lu, K.Y. Luo, Y.K. Zhang, C.Y. Cui, G.F. Sun, J.Z. Zhou, L. Zhang, J. You, K.M. Chen, J.W. Zhong, Grain refinement of LY2 aluminum alloy induced by ultra-high plastic strain during multiple laser shock processing impacts, Acta Materialia. 58, (2010), 3984–3994.

42. W. Pfeiffer, T. Frey, Strengthening of ceramics by shot peening, Journal of the European Ceramic Society. (2006), 2639–2645.

43. J.Z. Lu, K.Y. Luo, Y.K. Zhang, C.Y. Cui, G.F. Sun, J.Z. Zhou, L. Zhang, J. You, K.M. Chen, J.W. Zhong, Grain refinement of LY2 aluminum alloy induced by ultra-high plastic strain during multiple laser shock processing impacts, Acta Materialia. 58, (2010), 3984–3994.

44. L. C. Tshabalala, S. Pityana, Surface texturing of Si_3N_4–SiC ceramic tool components by pulsed laser machining, Surface and Coating Technology. 289, (2016), 52 – 60.

45. W. H. Gust, E. B. Royce, Dynamic yield strength of light armour materials, Metals, Ceramics, and Materials. TID-4500, UC-25. (1970), 1 -22.

46. Y. Liao., C. Ye., G. J. Cheng, A review: Warm Laser Shock Peening and Related Laser Processing Technique, Optics & Laser Technology, (78). (2016), 15 – 24.

47. C. Yang, P. Hodgson, Q. Liu, L. Ye., Geometrical effects on residual stresses, in 7050 – T7451 aluminium alloy rods subject to laser shock peening, Journal of Material Processing Technology, 201, (2008), 303 – 309.

48. K. A. Khor, Z. L. Dong, Y. W. Gu, Influence of Oxide mixtures on mechanical properties of plasma sprayed functionally graded coating, Thin Solid Film, 368 (1). (2000), 86 – 92.

49. J. Roy, S. Chandra, S. Das, and S. Maitra, Oxidation behaviour of Silicon Carbide – A Review, Review on Advance Material Science, 38, (2014), 29 – 39.

Citation for this Paper

Shukla, P., Nath, S., Wang, G., Shen, X. & Lawrence, J. **(**Aug 2017) **Surface property modifications of silicon carbide ceramic following laser shock peening,** Journal of the European Ceramic Society. 37**,** 9**,** p. 3027-3038 12 p.